

Total Electron Scattering Cross Sections for Cyclofluorobutane

Hiroyuki NISHIMURA* and Akira HAMADA[†]

The Gaseous Electronics Institute, Merria A-1303, 1-4 Onoye-cho, Kita-ku, Nagoya 462-0863

[†]*Computer Science, Junior College, Yamaguchi University, Daido, Hofu, Yamaguchi 747-12*

(Received July 5, 2006; accepted October 19, 2006; published December 25, 2006)

Total electron scattering cross sections for c-C₄F₈ have been measured in the energy range between 1 and 3000 eV using a compact linear-type electron transmission apparatus. Electrons scattered into a narrow forward angle were examined using some of the scattered currents and an empirical formula. The present results were compared with available theoretical and experimental data. Inelastic electron scattering cross sections were examined in the energy ranges of 1.5–7, 1.5–15, and 15–100 eV. The validity of the present results was examined. The most plausible electric dipole polarizability for c-C₄F₈ was chosen from the available data.

KEYWORDS: electron scattering, electron–molecule scattering, total cross section, c-C₄F₈

DOI: [10.1143/JPSJ.76.014301](https://doi.org/10.1143/JPSJ.76.014301)

1. Introduction

Cyclofluorobutane (c-C₄F₈) is a typical polyatomic molecule with a large electric dipole polarizability α ,^{1,2)} although it is without an electric dipole moment μ and an electric quadrupole moment.

On the other hand, c-C₄F₈ has received much interest among the material gases for etching plasma for silicon-based devices because of its excellent selectivity of SiO₂ on Si substrates.³⁾ Vinogradov *et al.*⁴⁾ showed that c-C₄F₈ is the most efficient material for the generation of CF₂ in fluorocarbon plasma. To understand the etching mechanism in the plasma, many theoretical and experimental studies were performed for the determination of electron scattering cross sections (the total and partial ionization cross sections, inelastic excitation cross sections and electron attachment cross sections).

Sanabia *et al.*⁵⁾ measured the total electron scattering cross sections (σ_T , 1–20 eV) using an improved linear electron transmission apparatus (ILET) with a trochoidal monochromator. Winstead and McKoy⁶⁾ presented the theoretical elastic and inelastic scattering cross sections in the low-energy range by the Schwinger multichannel method. The electron attachment cross sections (σ_a) were obtained by an electron beam experiment or by unfolding the electron-swarm experimental data. Chutjian and Alajajian⁷⁾ measured σ_a (0–170 meV) using their krypton photoionization technique. A typical σ_a (0–10 eV) from a swarm experiment was reported by Spyrou *et al.*⁸⁾ Recently, Jelisavcic *et al.*⁹⁾ have reported experimental elastic differential cross sections (DCSs, 1.5–100 eV), integral elastic scattering cross sections (σ_{el} , 1.5–100 eV) and differential vibrational excitation cross sections [DCS(vib)s, 1.5–7 eV]. Novak and Fr  chette¹⁰⁾ and Font *et al.*¹¹⁾ reported the vibrational excitation cross section (σ_v). Yamaji and Nakamura¹²⁾ modified the σ_v found by Itoh and Musha¹³⁾ using measured electron transport coefficients and their procedure. Toyoda *et al.*¹⁴⁾ measured partial ionization cross sections (threshold, 117.8 eV) and found that the cross sections dissociate into neutral fragments [neutral dissocia-

tion cross section, σ_d^n (Toyoda), threshold, 250 eV] using a quadrupole mass spectrometer built in a dual-beam device. Jiao *et al.*¹⁵⁾ reported experimental partial ionization cross sections (16–200 eV) using a mass spectrometer. Christophorou and Olthoff²⁾ reviewed electron scattering cross sections and proposed the recommended cross sections for each scattering process. Font *et al.*¹¹⁾ also presented a set of recommended cross sections including a Born-type expression for vibrational excitation and neutral dissociation.

Of these cross sections, the total electron scattering cross section and elastic electron scattering cross section are important as normalization standards for other related cross sections. However, only a few theoretical and experimental σ_T and σ_{el} can be used. The first objective of this work is to determine σ_T for c-C₄F₈ over a wide energy range. The second is to determine the behavior of electrons scattered in a narrow forward scattering angle range (hereafter abbreviated as the forward-scattered electrons) that is likely to aid in the clarification of the scattering mechanism. The third is to query the validity of the inelastic electron scattering cross sections that have been used to date.

2. Experimental Procedure

The experimental procedure was reported in detail previously.¹⁶⁾ Therefore, only matters that closely relate to this work will be described. The apparatus used in this study is the same as that used in the previous work. That is, a type of linear electron transmission (LET) apparatus, which is shown schematically in Fig. 1. The electron beam is collimated by a static lens system. The opening diameters of the apertures A₁–A₉ shown in the figure are 0.5, 1.0, 1.0, 0.6, 1.0, 1.4, 1.8, 2.4, and 5 mm, respectively. The total cross section is defined by the Beer–Lambert relation,

$$I = I_0 \exp(-N\sigma l), \quad (2.1)$$

where I is the transmitted current, I_0 is the incident current, N is the number density of the target gas and l is the effective electron scattering length. Here, l is longer than the geometrical length (2.78 cm) of the collision cell. The electrons scattered in the collision cell CC, scattered in the subcell SC and received in the Faraday cup FC are separately measured as I_c , I_s , and I_f , respectively, and are used for the determination of σ . Using measured currents

*E-mail: nishimrh@kb3.so-net.ne.jp

[†]Deceased.

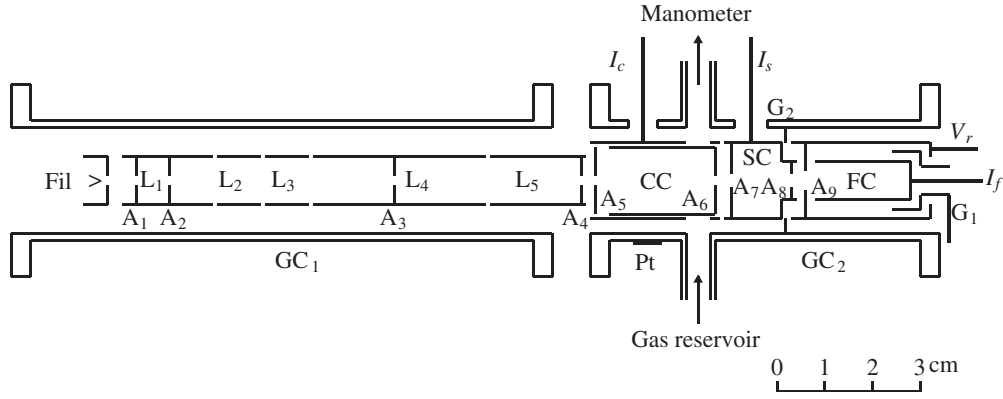


Fig. 1. Schematic of experimental apparatus.

and the target gas number density, l can be estimated. Corresponding to the geometrical length (2.78 cm) of CC and the effective electron scattering length, the provisional cross section σ_0 and the temporary cross section σ_t are determined, respectively.¹⁶⁾ Neither of these cross sections includes forward scattered electrons, which are measured as a part of I_f . For an estimation of the forward scattered electrons, the angular distribution of scattered electrons is assumed¹⁶⁾ to be

$$F(\theta) = G \frac{1}{[1 + A \sin^2(\theta/2)]^2}, \quad (2.2)$$

where G and A are energy-dependent coefficients. The coefficients G and A provide the absolute value and angular distribution of scattered electrons, respectively. These coefficients are determined using the average critical angles of electrons scattered in CC and SC. The cross sections corresponding to the forward scattered electrons (hereafter abbreviated as the forward scattering cross sections) are given by the integration of eq. (2.2) in the angular interval between the critical angles θ_i and θ_j . The integral cross section is given by $2\pi \int_{\theta_i}^{\theta_j} \sin(\theta) F(\theta) d\theta$. For example, the upper bound of the angle that views the entrance of the FC from any position on the central axis of CC is about 50 mrad in this study. Details were already provided in the previous report.¹⁶⁾ The forward scattering cross section is obtained by a combination of the electrons scattered in CC and SC. The determined coefficients A and G are shown in Fig. 2. The resultant forward scattering cross section is denoted simply as $\delta\sigma^{(n+1)}$.

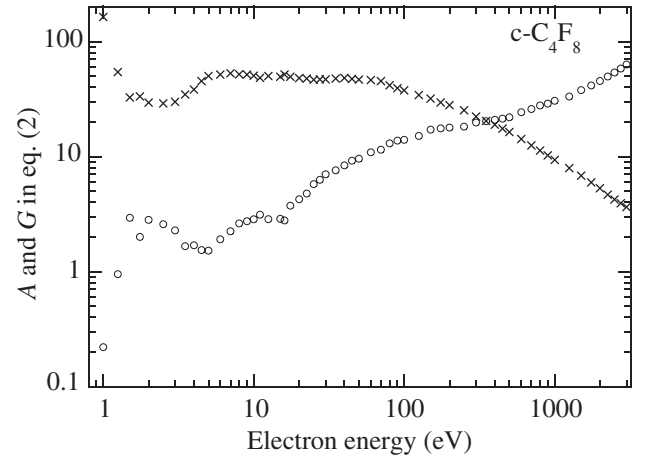
Corresponding to this cross section, the electron scattering length is given as $\delta l^{(n+1)}$. This value includes the proper length δl_0 of the target gas that effuses from CC to SC. Practically, δl_0 is determined as a minimum value under the condition $A \geq 0$ in eq. (2.2). In this case, δl_0 is 0.45 cm. The final total cross section is given as

$$\sigma_T = \sigma_t + \delta\sigma^{(n+1)}. \quad (2.3)$$

As shown previously,¹⁶⁾ a simple expression can be fitted to σ_T in a limited energy range:

$$\sigma_T = \text{const.} E^b, \quad (2.4)$$

where E is the incident electron energy and b is a parameter. The slope of σ_T is characterized by the parameter b . This value is used for the evaluation of the uncertainty in incident

Fig. 2. Experimentally determined coefficients in eq. (2.2) vs electron energy. Open circles: A ; crosses: G .

electron energy.

The systematic uncertainty includes the accuracy of the electron current meters, the manometer, the geometrical length of CC, the purity of the target gas, the energy width of the incident electron beam and the voltage attenuator that is used for the determination of incident electron energies higher than 1 keV. The total uncertainty is defined as the quadratic sum of the statistical and systematic uncertainties. As a first step, the energy scale of the incident electron beam was determined by comparing the position of the He 19.3 eV resonance profile in pure He with that in $c\text{-C}_4\text{F}_8$ diluted by He. The displacement of the electron energy between the former and the latter was 0.80 eV. The dependence of I_c on the target gas pressure was examined at an electron energy of 50 eV. For the measurements, a typical target gas pressure in CC was about 4×10^{-2} Pa. The purity of the target gas was 99.99%. During the measurements, the background pressure of the vacuum vessel was maintained below 2.7×10^{-4} Pa.

3. Results and Discussion

Well-converged values (deviation $\leq 0.0023\%$) of $\delta\sigma^{(n+1)}$ and $\delta l^{(n+1)}$ were obtained at $n = 5$. Therefore, $\delta\sigma^{(6)}$ is used instead of $\delta\sigma^{(n+1)}$ in eq. (2.3). The temporary total cross sections σ_t and the final total cross sections σ_T are listed in Table I with the total uncertainty.

Figure 3 shows the cross sections σ_0 , σ_t , $\delta\sigma^{(6)}$ and σ_T

Table I. Total electron scattering cross sections for c-C₄F₈ (10⁻²⁰ m²). (σ_i : without any forward scattering correction, σ_T : including $\delta\sigma^{(6)}$ and σ_i). Numbers in parentheses include both systematic and statistical uncertainties (%).

E (eV)	σ_i	σ_T	E (eV)	σ_i	σ_T
1	29.3	29.6(6.2)	50	41.4	44.3(4.3)
1.25	26.3	26.6(4.9)	60	41.5	44.7(4.3)
1.5	24.1	24.7(4.9)	70	40.8	44.1(4.3)
1.75	22.1	22.5(4.5)	80	37.8	41.2(4.5)
2.0	21.5	22.1(4.5)	90	35.8	39.2(4.4)
2.5	20.7	21.2(4.3)	100	34.3	37.6(4.6)
3.0	20.6	21.1(4.4)	125	31.4	34.6(4.6)
3.5	21.5	21.9(4.3)	150	29.3	32.7(4.6)
4.0	23.8	24.3(4.3)	175	27.2	30.3(4.6)
4.5	27.2	27.7(4.3)	200	25.8	28.8(4.7)
5.0	30.0	30.5(4.3)	250	23.3	26.1(4.7)
6.0	33.6	34.2(4.3)	300	20.6	23.2(4.9)
7.0	36.3	37.1(4.3)	350	18.9	21.3(4.9)
8.0	37.2	38.1(4.4)	400	17.5	19.8(4.9)
9.0	37.4	38.4(4.4)	450	16.2	18.4(4.9)
10	37.1	38.0(4.4)	500	15.1	17.2(5.0)
11	36.3	37.3(4.4)	600	13.2	15.2(5.3)
12.5	36.7	37.7(4.3)	700	11.6	13.5(5.3)
15	36.3	37.3(4.3)	800	10.5	12.3(5.3)
16	37.8	38.7(4.3)	900	9.50	11.2(5.3)
17.5	38.6	39.8(4.3)	1000	8.69	10.3(5.3)
20	38.5	39.9(4.3)	1250	7.39	8.87(5.4)
22.5	38.9	40.4(4.3)	1500	6.33	7.75(5.5)
25	39.1	40.8(4.3)	1750	5.54	6.89(5.5)
27.5	39.9	41.8(4.3)	2000	4.92	6.20(5.6)
30	40.5	42.6(4.3)	2250	4.33	5.54(5.7)
35	41.5	43.9(4.4)	2500	3.93	5.10(5.8)
40	42.4	44.9(4.3)	2750	3.63	4.79(5.8)
45	41.9	44.6(4.3)	3000	3.36	4.50(5.8)

obtained at various experimental phases as functions of electron energy. The phases were discussed in §2. The distribution of $\delta l^{(6)}$ with respect to electron energy shows its minimum, to be around 1 eV, which offers a clue for the effective electron scattering length in SC. The energy dependence of $\delta\sigma^{(6)}$ is emphasized by the energy dependence of the coefficient A in Fig. 2.

3.1 TCS

The proportionality between σ_T for electrons at high energies and the total number of electrons (z) in a molecule is known.¹⁷⁾ This relationship can be used for the assessment of σ_T . The typical values of σ_T/z for several molecules are summarized in Table II. Regardless of the chemical structure, the values of σ_T/z show a trend where they approach a common value in the high-energy range. Therefore, the present results seem reasonable for high-energy electrons. The relationship between σ_T and α is not considered here because many values are reported for the electric dipole polarizability of c-C₄F₈.^{1,2)} Plausible α values are discussed later.

σ_T values are compared with available theoretical and experimental data in Fig. 4. The results of Sanabia *et al.*⁵⁾ are considerably larger than our results at energies below

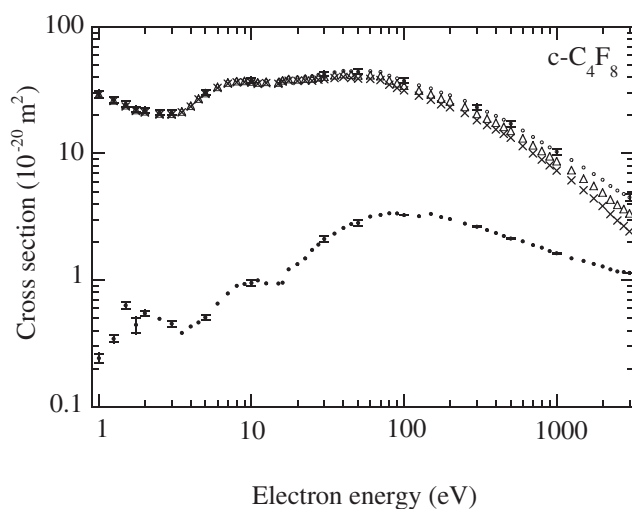


Fig. 3. Scattering cross sections for c-C₄F₈ at various experimental phases vs electron energy. Open circles: σ_T ; open triangles: σ_i ; cross: σ_0 ; solid circles: $\delta\sigma^{(6)}$.

Table II. σ_T/z .

E (eV)	CF ₃ H ^{a)}	CF ₄ ^{b)}	C ₃ F ₈ ^{b)}	CF ₃ I ^{a)}	c-C ₄ F ₈
30	0.70	0.47	0.44	0.48	0.44
100	0.49	0.42	0.40	0.33	0.39
500	0.20	0.18	0.18	0.13	0.18
700	0.16	0.15	0.15	0.12	0.14
1000	0.12	0.11	0.11	0.09	0.11
3000	0.051	0.048	0.053	0.044	0.047

a) Ref. 16. b) Ref. 18.

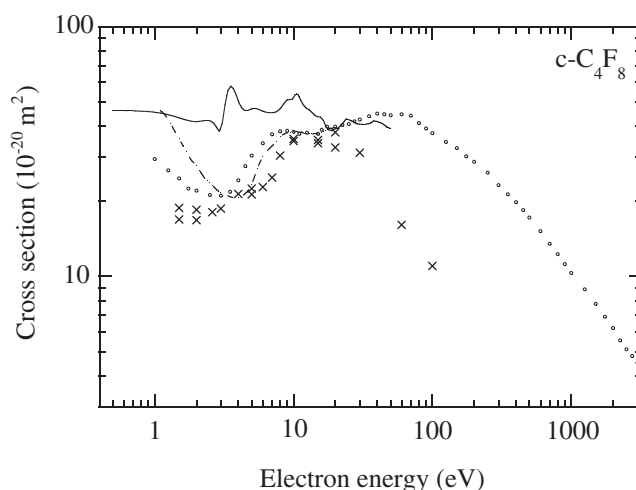


Fig. 4. Available total and elastic electron scattering cross sections vs electron energy. Open circles: this work; dotted line: Sanabia; crosses and pluses: Jelisevic; solid line: Winstead.

3 eV. An energy shift of about 0.8 eV is found at the minima between their results and our results in this energy range. The agreement between these two results is excellent at energies higher than 8 eV. Jelisevic *et al.* reported differential elastic cross sections (DCSS, 1.5–100 eV) and integral elastic cross sections (σ_{el} , 1.5–7 eV). Their results for σ_{el} are

nearly the same as σ_T for electron energies of 3, 10, and 16 eV. The theoretical results of Winstead and McKoy⁶⁾ agree well with our results for electron energies higher than 20 eV. They predicted the positions of many shape resonances. However, their results are larger than our results in the energy range below 20 eV.

3.2 Forward electron scattering

The energy dependence of $\delta\sigma^{(6)}$ shows some structure that may correspond to a proper scattering process, as shown in Fig. 3. A clear peak and a broad hump can be seen at 2 and 10 eV in $\delta\sigma^{(6)}$, respectively. The peak at 2 eV is not found for σ_T . σ_T decreases monotonically with increasing electron energy, whereas $\delta\sigma^{(6)}$ increases for electron energies in the range of 1–2 eV. This trend is different from those for polar molecules.¹⁶⁾ The ratio $\delta\sigma^{(6)}/\sigma_T$ is about 3% or less for electron energies of 1–20 eV. This fact seems to indicate that the angular distribution of scattered electrons has no marked intensity distribution in a narrow forward angle range. On the contrary, for electrons with energies higher than 25 eV, it is not possible to disregard some the forward scattered electrons in σ_T .

3.3 σ_T , σ_{el} , and σ_v^{eb} at 1.5–7 eV

Jelisavcic *et al.* reported σ_{el} for electron energies from 1.5 to 100 eV. The inelastic scattering cross section can be evaluated by subtracting σ_{el} ⁹⁾ from σ_T . Here, this is referred to as the presumed inelastic scattering cross section (σ_{inel}^{psm}). Jelisevic *et al.* also reported vibrational differential excitation cross sections (DCS(vib)s, 1.5–7 eV). The integral vibrational excitation cross sections σ_v^{eb} are estimated from their measured DCS(vib) in this study. Figure 5 shows σ_T , σ_{el} (Jelisavcic), σ_v^{eb} , and σ_{inel}^{psm} for electron energies of 1.5–7 eV. As can be seen, σ_T and σ_{el} ⁹⁾ are almost the same for electron energies of 3–3.5 eV. Jelisevic *et al.* did not observe any marked inelastic processes other than the vibrational excitation in the elastic DCS measurement. Therefore, the vibrational excitation is the predominant inelastic scattering process in this narrow energy range. However, for energies below 3 eV or above 4 eV, σ_{inel}^{psm} is

considerably larger than σ_v^{eb} . Details of the inelastic electron scattering process other than the vibrational excitation are not clear in this energy range.

In this study, the coefficient b in eq. (2.4) was estimated to be about -0.5 at 1–2 eV. Vogt and Wannier¹⁹⁾ discussed the scattering of charged particles by a pure polarization potential and presented a formula proportional to $E^{-0.5}$ as the scattering cross section, which is interesting in its relationship with the coefficient b , although this is an extreme example. Chutjian and Alajajian⁷⁾ presented an empirical formula for σ_a for c-C₄F₈ that provides the main term with $E^{-0.5}$. Their expression was established for very low energy electrons (0–0.17 eV). Therefore, it seems that it is difficult to estimate σ_a in this energy range using their formula. On the other hand, available σ_a ²⁾ values are insufficient as candidates for σ_{inel}^{psm} because they are too small.

For the understanding of the result of $b \simeq -0.5$ in eq. (2.4) and the large value of σ_T in this energy range, the available data is not sufficient.

3.4 σ_{inel}^{psm} and σ_v at 1.5–15 eV

The presumed inelastic scattering cross sections discussed in the above section are extended up to the ionization threshold. They are compared with the available vibrational excitation cross sections in Fig. 6. Results of Itoh and Musha, Novak and Fréchet, Font *et al.*, and Yamaji and Nakamura are denoted as σ_v (Itoh), σ_v (Novak), σ_v (Font) and σ_v (Yamaji), respectively. All σ_v values cited were obtained from the electron swarm experiments, except σ_v^{eb} . This figure also includes σ_d^n (Font) values that were obtained from eq. (6) in ref. 11 and σ_a (Christophorou). The cross sections σ_{inel}^{psm} exhibit a broad bottom and a hump at electron energies of 3 and 6 eV, respectively. The bottom at 6 eV and two humps at 2 and 9 eV can be seen in σ_v (Yamaji). Yamaji and Nakamura attributed the hump appearing in the lower electron energy range to the vibrational resonance excitation of the C–C bond and the other hump in the higher range to the same mechanism for the C–F bond in the target

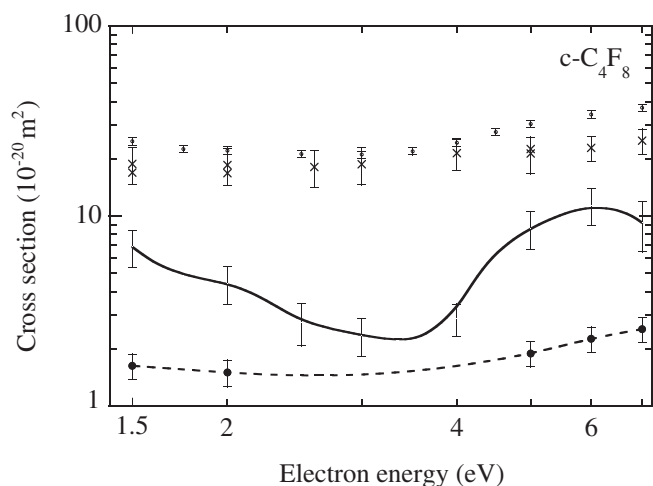


Fig. 5. Presumed inelastic scattering cross section vs electron energy. Open circles: σ_T ; crosses: σ_{el} (Jelisavcic); dotted line and solid circles: σ_v^{eb} ; solid line: σ_{inel}^{psm} .

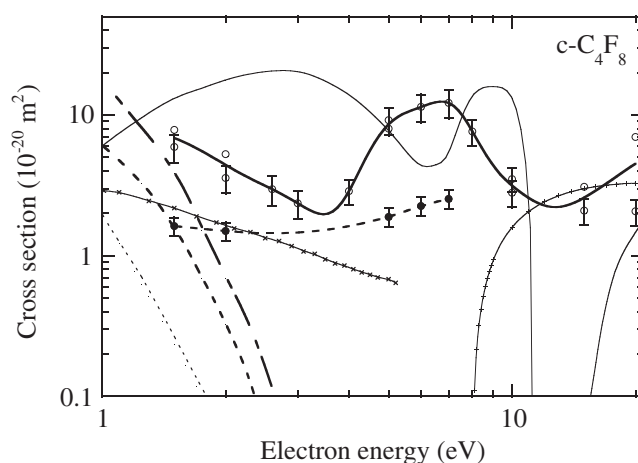


Fig. 6. Presumed inelastic scattering cross section vs electron energy. Solid line: σ_{inel}^{psm} ; open circles: $\sigma_T - \sigma_{el}$ (Jelisavcic); solid circles and dotted line: σ_v^{eb} ; short line and dots: σ_v (Itoh); dotted line: σ_v (Novak); thin solid line: σ_v (Yamaji); crosses and thin line: σ_v (Font); pluses and thin line: σ_d^n (Font); fine dots: σ_a (Christophorou); dots and thin line: σ_l (Jiao).

molecule. The magnitude and energy width reported by Yamaji and Nakamura are similar to those for this work but their results appeared at an energy about 3 eV higher than that of our results. If their energy setting is shifted to lower energies by 3 eV, the hump and the bottom agree well with those in $\sigma_{\text{inel}}^{\text{psm}}$. On one hand, the DCS(vib) measured by Jelisivcic *et al.* did not show such a large shift in the electron energy range of 1.5–7 eV. The contribution of $\sigma_a^{2,8)}$ to $\sigma_{\text{inel}}^{\text{psm}}$ is not considered in this case because it is too small in comparison with σ_v^{eb} . The reason for the discrepancy between σ_v^{eb} and σ_v (Yamaji) is not clear. Both σ_v (Itoh) and σ_v (Novak) show different energy dependences from σ_v^{eb} in the energy range considered. A good agreement can be seen between σ_v (Font) and σ_v^{eb} for electron energies of 1.5–3 eV, while the disagreement between those results increases with increasing electron energy. The agreement between $\sigma_{\text{inel}}^{\text{psm}}$ and σ_d^n (Font) is good at energies higher than 10 eV. Therefore, $\sigma_{\text{inel}}^{\text{psm}}$ for electron energies of 10–15 eV may be attributed to the neutral dissociation cross sections.

3.5 $\sigma_{\text{n-inel}}^{\text{psm}}$ at 15–100 eV

The inelastic electron scattering cross section without ionization (hereafter abbreviated as the neutral inelastic electron scattering cross section) is defined as

$$\sigma_{\text{n-inel}}^{\text{psm}} = \sigma_T - \sigma_{\text{el}} - \sigma_I, \quad (3.1)$$

where σ_{el} and σ_I are quoted from refs. 9 and 15, respectively. Toyoda *et al.*¹⁴⁾ measured σ_d^n (Toyoda). Font *et al.*¹¹⁾ also reported the total neutral dissociation cross sections σ_d^n (Font). The estimated $\sigma_{\text{n-inel}}^{\text{psm}}$ and the cross sections related to it are shown in Fig. 7. The magnitudes of $\sigma_{\text{n-inel}}^{\text{psm}}$ and σ_I are comparable as long as these cross sections are used for electron energies of 20–100 eV. The agreement between $\sigma_{\text{n-inel}}^{\text{psm}}$ and σ_d^n (Font) is very good for electron energies of 15–30 eV. However, considerable discrepancy can be observed between the above two cross sections in the energy range higher than 30 eV. The electronic excitation (without the ionization) processes corresponding to such large values of cross sections were not reported.

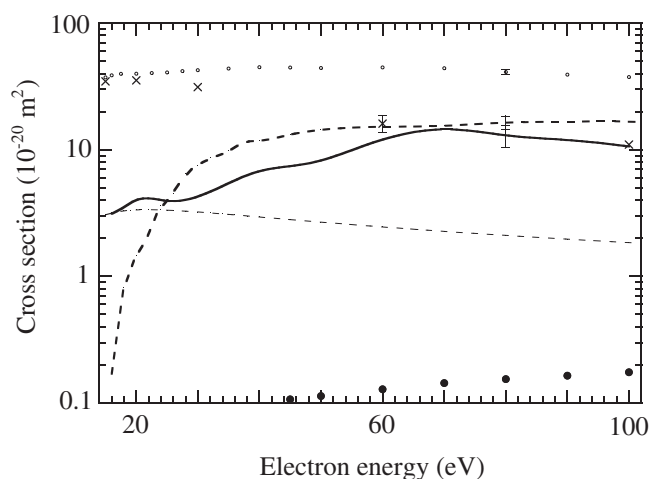


Fig. 7. Presumed neutral inelastic scattering cross section vs electron energy. Open circles: σ_T (this work); thin dotted line: σ_d^n (Font); crosses: σ_{el} (Jelisivcic); solid circles: σ_d^n (Toyoda); dotted line: σ_I (Jiao); solid line: $\sigma_{\text{n-inel}}^{\text{psm}}$.

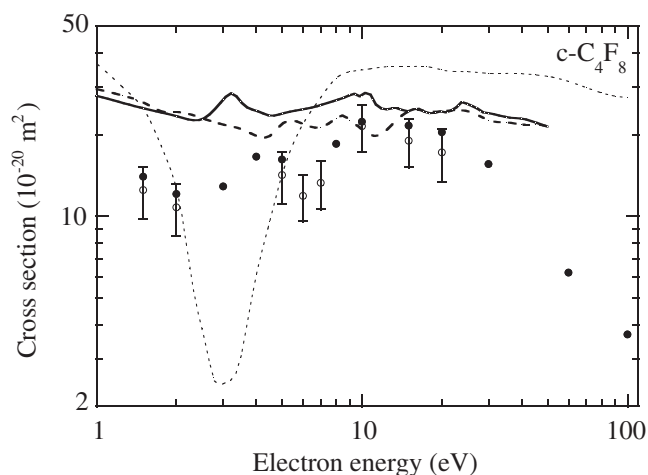


Fig. 8. Momentum transfer cross section vs electron energy. Open circles and solid circles: Jelisivcic; dotted line: Font; fine dotted line: Yamaji; solid line: Winstead.

Generally, the main part of σ_T is composed of σ_{el} and σ_I . Such large values of $\sigma_{\text{n-inel}}^{\text{psm}}$ for electron energies higher than 30 eV seem to have some problems in the related cross sections. Let us examine σ_{el} using the momentum transfer cross section (σ_{MT}), temporarily, because the electron swarm experiment determines σ_{MT} instead of σ_{el} . Figure 8 shows the energy dependence of σ_{MT} obtained by various methods. The method of Font *et al.*¹¹⁾ and Yamaji and Nakamura¹²⁾ is based on the electron swarm experiment. Jelisivcic *et al.*⁹⁾ used an electron beam experiment. Winstead and McKoy⁶⁾ obtained the result by theoretical calculation. The energy dependence of σ_{MT} found by Font *et al.*, Yamaji and Nakamura, and Winstead and McKoy resembles that for electron energies higher than 10 eV. On the other hand, the σ_{MT} of Jelisivcic *et al.* and that of Winstead and McKoy differ in magnitude and inclination for electron energies higher than 20 eV. A situation that appears similar to this was observed in Fig. 4. Such a difference may be an effect of the cross section obtained from the electron beam experiments. In the electron beam experiments, DCS in the forward scattering and back scattering angles is calculated by extrapolation to obtain the integral cross section. The magnitude of the σ_{el} of Jelisivcic *et al.* seems to be too small for electrons with energy of 20 eV or higher. On the other hand, σ_d^n (Toyoda) is very small compared with $\sigma_{\text{n-inel}}^{\text{psm}}$.

3.6 Electric dipole polarizability α

Electric dipole polarizability is an important physical constant for electron scattering from molecules. α has not yet been established although much theoretical and experimental data^{1,2)} is available. Therefore, it is sensible to choose a numerical value that seems to be the most certain. The proportionality between σ_T at high energies and α is known,²⁰⁾ which is useful for this purpose. Typical values of σ_T/α for several molecules are summarized in Table III, in which three values for $\text{c-C}_4\text{F}_8$ are presented as typical data. As in the case of the σ_T/z shown in Table II, the numbers in a line show a trend that converges to a common value for electrons at high energies. Therefore, as long as the above criterion is admitted, $9.24 \times 10^{-30} \text{ m}^3$ can be chosen as α for this molecule.

Table III. σ_T/α .

E (eV)	$\text{CF}_3\text{H}^{\text{a}}$	CF_4^{b}	$\text{C}_3\text{F}_8^{\text{b}}$	$\text{CF}_3\text{I}^{\text{a}}$		$\text{c-C}_4\text{F}_8$	
30	6.7	5.2	4.3	5.2	5.8	4.6	4.1
100	4.8	4.6	3.8	3.6	5.1	4.1	3.6
500	1.9	2.0	1.8	1.5	2.3	1.9	1.6
700	1.5	1.6	1.4	1.3	1.8	1.5	1.3
1000	1.1	1.2	1.1	1.0	1.4	1.1	0.99
3000	0.50	0.52	0.51	0.48	0.61	0.49	0.43
α (\AA^2)	3.52 ^{c)}	3.838 ^{c)}	9.4 ^{d)}	7.97 ^{d)}	7.37 ^{e)}	9.24 ^{e)}	10.4 ^{d)}

a) Ref. 16. b) Ref. 18. c) Ref. 20. d) Ref. 1. e) Ref. 2.

4. Conclusions

The energy dependence of the electron scattering cross sections ($\sigma_T, \delta\sigma^{(6)}$) in the low-energy range may be due to the features (large α , without μ) of the molecule. The total electron scattering cross sections for c-C₄F₈ reported by Sanabia *et al.*⁵⁾ are considerably larger than the present results in the low-energy range. However, if the electron energy setting of their results is shifted to lower energies by 0.8 eV, agreement between these two results is excellent. The necessity for an extra inelastic excitation cross section was indicated for the energy range of 1.5–15 eV. The excessive total inelastic excitation cross sections without ionization were estimated with available data and the present results for electron energies of 15–100 eV. Those values seem to be slightly larger than expected. In other words, either or both of the elastic scattering cross sections and the total ionization cross sections seem to be smaller than the expected values. From a considerable amount of theoretical and experimental data, an electric dipole polarizability of $9.24 \times 10^{-30} \text{ m}^3$ is the most acceptable for this work. The validity of the measured results was examined on the basis of the fact that the total electron scattering cross section depends on the total number of electrons in a molecule for high-energy electrons.

Many reliable and systematic electron scattering cross

sections for c-C₄F₈ are needed not only to understand the scattering process but also to promote the applied and related fields.

Acknowledgments

We would like to express our gratitude to Professor Nakamura for permission to use the facilities in his laboratory. We also would like to thank Professor Itikawa for advice and many comments.

- 1) J. A. Beran and L. Kevan: *J. Phys. Chem.* **73** (1969) 3860.
- 2) L. G. Christophorou and J. K. Olthoff: *J. Phys. Chem. Ref. Data* **30** (2001) 449.
- 3) W. W. Stoffels, E. Stoffels, and K. Tachibana: *J. Vac. Sci. Technol. A* **16** (1998) 87.
- 4) I. P. Vinogradov, A. Dinkelmann, and A. Lunk: *J. Phys. D* **37** (2004) 3000.
- 5) J. E. Sanabia, G. D. Cooper, J. A. Tossel, and H. Moore: *J. Chem. Phys.* **108** (1998) 389.
- 6) C. Winstead and V. Mckoy: *J. Chem. Phys.* **114** (2001) 7407.
- 7) A. Chutjian and S. H. Alajajian: *J. Phys. B* **20** (1987) 839.
- 8) S. M. Spyrou, S. R. Hunter, and L. G. Christophorou: *J. Chem. Phys.* **83** (1985) 641.
- 9) M. Jelisavcic, R. Panajotovic, M. Kitajima, M. Hoshino, and H. Tanaka: *J. Chem. Phys.* **121** (2004) 5272.
- 10) J. P. Novak and M. F. Fr  chette: *J. Appl. Phys.* **63** (1988) 2570.
- 11) G. I. Font, W. L. Morgan, and G. Mennenga: *J. Appl. Phys.* **91** (2002) 3530.
- 12) M. Yamaji and Y. Nakamura: *J. Phys. D* **37** (2004) 1525.
- 13) T. Itoh and T. Musha: *J. Phys. Soc. Jpn.* **15** (1960) 1675.
- 14) H. Toyoda, M. Ito, and H. Sugai: *Jpn. J. Appl. Phys.* **36** (1997) 3730.
- 15) C. Q. Jiao, A. Garscadden, and P. D. Haarlund: *Chem. Phys. Lett.* **297** (1998) 121.
- 16) H. Nishimura and Y. Nakamura: *J. Phys. Soc. Jpn.* **74** (2005) 1160.
- 17) K. Floeder, D. Fromme, W. Raith, A. Schwab, and G. Sinapius: *J. Phys. B* **18** (1985) 3347.
- 18) H. Nishimura, F. Nishimura, Y. Nakamura, and K. Okuda: *J. Phys. Soc. Jpn.* **72** (2003) 1080.
- 19) E. Vogt and G. H. Wannier: *Phys. Rev.* **95** (1954) 1190.
- 20) Cz. Szmytkowski: *Z. Phys. D* **13** (1989) 69.
- 21) *Handbook of Chemistry and Physics*, ed. D. R. Lide (CRC Press, Boca Raton, 2001) 82nd ed.